Research Article

Cnn-Based Palm Vein Confirmation In An Integrated Biometrics Id Configuration

Komal Teotia[1], Dr. Manav Bansal[2]

[1] Scholar M.Tech CSE, SCRIET, Chaudhary Charan Singh University, Meerut, India
[2] Assistant Professor, SCRIET, Chaudhary Charan Singh University, Meerut, India

ARTICLE INFO	ABSTRACT
	Lately, automated biometric recognizing evidence system has wide applications including modified ID and data get, which integrates customized security checking, affirming individual character to forestall information divulgence or character coercion, and so forth. With the movement of biotechnology, recognizing verification structures considering biometrics have emerged keeping watch. These systems require high precision and ease of use. Palm vein conspicuous confirmation is a sort of biometric that perceives palm vein features. Differentiated and various features, palm vein affirmation gives definite results and has gotten noteworthy thought. It encouraged a cunning unrivalled execution and noncontact palm vein affirmation system by using better execution flexible establishment filtering than obtain palm vein photos of the locale of interest. After that, at that point, used a changed convolution mind association to conclude the best affirmation model through getting ready and testing

1.Introduction

The process of identifying people by their distinct biological traits is known as biometrics. As such, possible issues like forgotten passwords can be resolved with the application of digital biometric technologies. Numerous biometric techniques, including identification of faces [1], identification of fingerprints [2], palm print identification [3], recognition of the iris [4], and palm vein recognition [5], have been proposed. Typically, a visible light camera is used to take pictures for facial recognition systems. Nevertheless, the procedure is vulnerable to changes in the face's position or an unreliable light source. In addition, as a person ages, recognition problems could happen. There is a sweat and dirt sensitivity to fingerprint and palm print recognition algorithms. Recognition accuracy is impacted by poorly captured texture features. Despite the excellent accuracy of iris recognition, users may find it uncomfortable when their iris is scanned by infrared cameras. The biological traits of the aforementioned identification techniques are exterior aspects that are easily replicable by malevolent actors, which is a common drawback.

The size and cost of the equipment are also important elements that influence a system's viability. Palm veins are more stable than other identifying methods since they are concealed beneath the skin and cannot be faked. Features that remain the same as a person ages can be captured with small camera equipment. Every person has a different structure to their palm veins. The textures of palm veins vary even among twins. Data for identification based on biological properties of the palm vein are relatively safe and trustworthy in a large database when compared to other biological characteristic-based identification approaches.

The majority of newly developed corpse identification systems use bioinformatics. One of the things that prevent people from using biometric systems is the size of most of their devices. Lowering the cost, raising the recognition rate, and quickening response time are the primary requirements for growing use. Low-cost devices, however, only record images with low resolution, which results in poor quality images. The system's reaction time and identification stability decrease in a big database, raising the complexity of characteristic

identification and making the system impractical for real-world use. Consequently, techniques for identifying palm veins have been put forth to get around these issues.
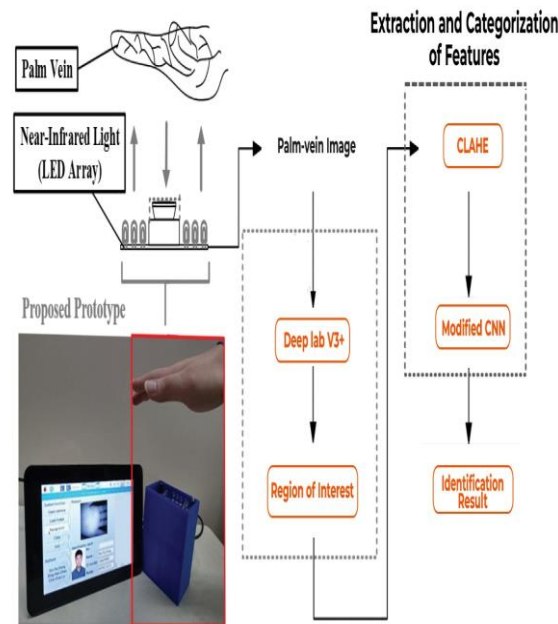

Figure 1: The proposed Palm vein identification systems schematic diagram and device protype are shown on the bottom left.

An infrared imaging device was employed by Lin et al. [6] to acquire images of the hand veins. Despite having good image quality, the equipment is too expensive. In order to show the red blood cells in the finger, Toh et al. [7] suggested using a common, inexpensive network camera as an image capture tool. This camera used near-infrared light, which has a wavelength between 600 and 1000 nm. An infrared filter is placed in front of the camera lens to block out visible light in order to prevent the influence of ambient light sources. However, the issue of uneven contrast reduces the recognition rate of infrared light due to its tendency to scatter. A multi-scale filtering scheme was used by Zhang et al. [8] to extract palm vein features. To improve recognition stability, Lee et al. [9] suggested applying a 2-D Gabor filter; nevertheless, this requires a large computation time to identify the region where the palm is distinguished from the background. Furthermore, the features of palm vein and palm print tend to be mixed because in [9] the near-infrared LED used has a wavelength of 750 nm. A feature fusion algorithm utilizing a near-infrared camera system was presented by Han et al. [10]. Despite the high recognition rate, the camera system is bulky and difficult to relocate. Scale Invariant Feature Transform (SIFT) algorithm was suggested by Ladoux et al. [11] for identification, and it showed good identification based on twenty-four testers. To accurately extract the features of the palm vein, Mirmohamadsadeghi et al. [12] proposed the use of a Local Directional Pattern (LDP) feature extraction method. However, the recognition rate sharply drops when the features are shifted. A novel palm vein recognition system using a combination of Maximum Principle Curvature (MPC) and Local Binary Pattern (LBP) for feature extraction was presented by Kang et al. [13]. Such a double authentication technique allows for a strong matching performance. But there's a lot of computational complexity. A Region of Interest (ROI) algorithm was proposed by Ma et al. [14]; it increases the recognition rate by capturing the largest area to extract features. However, since it relies on iterations, it is unlikely to be applied in an inexpensive embedded platform. A novel recognition rate improvement algorithm (ROI) was proposed by Ma et al. [14] that capture the largest area features. But it isn't appropriate for realistic, low-cost embedded platform applications because of the numerous iterations in the search process, the enormous computational complexity, and the hardware implementation's high cost and high memory requirements.

By requiring users to touch the device with their palms, current public identification devices lessen health risks associated with direct contact with multiple people. With the addition of high-performance adaptive background filtering, this study suggested an enhanced deep learning (DL) method. Furthermore, the suggested approach achieves three benefits, employs contact-free equipment, and resolves the previously mentioned issues. The following are the main features: 1) one-to-many recognition; 2) real-time processing; and 3) high recognition rate.

2. Design for Provided Palm Vein Acceptance

A representation of the suggested palm vein verification system is shown in Figure 1. The computer vision techniques that have been shown in multiple studies were improved upon by this study.

Ultimately, the developed methodology was applied using cloud computing technology on the Raspberry Pi embedded platform. There are three components to the research method: 1) creation of the palm vein equipment architecture; 2) preliminary processing of images, incorporating Deeplab v3+ and region of interest; and 3) adjustment of the convolutional neural network (CNN).

2.1 Equipment Architecture of Palm vein verification system:

A 940 nm near-infrared (NIR) luminescent diode collection was placed next to a lens for this research, and it was subjected to toward radiation (the same direction as the lens was shot).The red blood cells in the veins receives the NIR light when it enters the blood vessels and creates an outline. This principle allows us to obtain NIR pictures of the palm veins, as shown in Fig. 2(a).

2.2 Preliminary Processing of Images

The device's noncontact requirement is met because palm vein images are taken with an inexpensive (low-resolution) camera. The obtained image quality is usually noisy and cluttered with extraneous background details, which makes it challenging to apply the DL algorithm later on. For this reason, efficient image preprocessing is especially important for biometrics research.

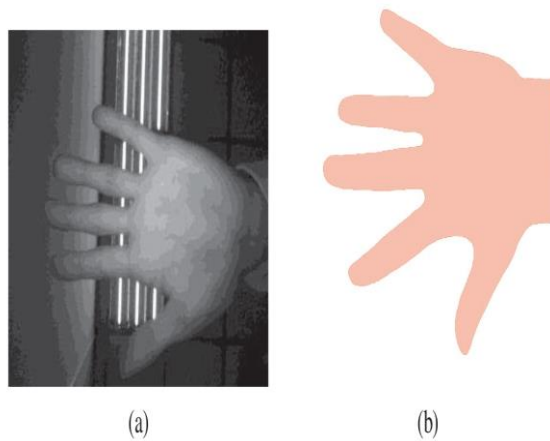(a)   (b)

Figure 2: An example of segmenting the palm vein background. (a) The picture of the palm vein that the suggested system took. (b) The segmented image of the palm vein.

Furthermore, background noise is usually present in the palm vein images that are taken due to the noncontact apparatus. Otsu thresholding is used in the conventional palm shape extraction technique [12, 13] to obtain hand lines.

But there is complexity to this method. Background noise and ambient light sources can lead to positioning errors in the background. Thus, this study proposed an extremely effective adaptive background sorting technique centered on DeepLabv3 [15] that performs conceptual surroundings classification using the encoder-decoder model. The architecture of this model is briefly described in the section that follows.

2.2.1 Encoder

It has a deep convolutional neural network (DCNN) with the largest pooling layer for hierarchical feature extraction and sampling, atrous convolution, and convolutional structures of various scales. The correlation between the one-dimensional signal input A[j] and the corresponding output hole convolution B[j] under a one-dimensional signal, a filter X[k] of size K, can be defined as follows:

$$B[j] = \sum_k^K A[j + r.k]X[k], \qquad\qquad\qquad (1)$$

Where the attribute r is the remove steps and the traditional convolution smaller value is set to a single one.

2.2.2 Decoder

It starts by bilinear increased sampling the encoder-provided image features, then moves on to a 1x1 and 3x3 convolutional layer. Ultimately, as illustrated in Fig. 2(b), the categorized palm vein image can be obtained by four time's bilinear increased sampling.
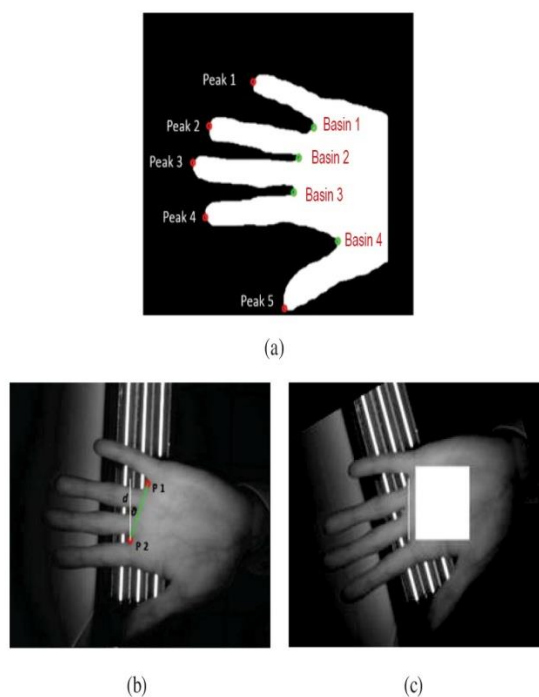
Examples of the ROI extraction from palm veins. (a) An explanation of the four finger basins and the five fingertip tips. (b) The angle θ that separates the finger basin segment from the vertical line. (c) Image of the normalized palm vein.

Figure 3 shows the diagram for the region of fascination (ROI) technique for studying the palm vein. To locate the ROI once the disturbance has been filtered. Firstly, the wrist is filtered in the picture to lessen the effect of extended sleeves on the hand or handheld devices like watches. The locations of the basin and peaks (fingertips) are then determined. The palm center of gravity is used as the origin when calculating the Euclidean distance between the palm edge and the center of gravity. The lowest point of the four regions and the highest point of the five regions are then determined. Fingertip peaks range from 1 to 5, while finger basin are shown as basin from 1 to 4. One can locate the palm area's size by utilizing basin 1 and 3. To ensure that the photos taken are not too big to extract information on features other than palm veins, the distance between basin 1 and 3 has been suitably increased.

to designate basin 1 as t1, basin 3 as t2, the distance between t1 and t2 as d, and the angle between the straight line and the vertical line as, as illustrated in Fig. 3(b). In order to get consistent palm vein features, the segmented palm vein image is rotated based on θ in order to solve the rotation problem. In (2) and (3), the relationship between d and θ is defined

$$d=\sqrt{(x_{t2}-x_{t1})^2-(y_{t2}-y_{t1})^2} \quad (2)$$
$$\theta=\tan^{-1}(x_{t2}-x_{t1}/y_{t2}-y_{t1}) \quad (3)$$

2.2.3 Improvement and Isolation of Features:
Depending on the user's angle and the stability of the light source, each image that the camera takes may have a different contrast. Consequently, as shown in Figure 4, to increased the dynamic range of the palm vein image by applying the contrast limited adaptive histogram equalization (CLAHE) algorithm.
By emphasizing the vein features, this algorithm can enhance the contrast of the image and extract the features, enabling the CNN to produce better classification results.

Convolutional neural network modification
The traditional VGG16 model was cited in this study [16]. An input layer, 14 convolutional layers, five Max pooling layers, one fully connected layer within each convolutional layer, a fully connected layer, and an output layer make up the suggested CNN architecture. It also included the SoftMax activation function and rectified linear unit (ReLU).
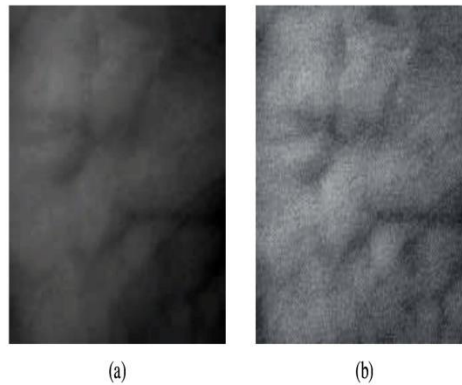
Figure 4 : An illustration of using CLAHE to improve the palm vein feature. (a)
Enter the palm vein ROI picture. (b) A better image of the palm vein.

Here is how the detailed architecture is displayed.

- **IN** The input layer contains the data of [160×160×1]. To change the original data size of [222×222×3] of VGG16 to the size more suitable for the characteristics of veins, which avoids the input data being deformed due to enlargement and reduction. In addition, the conversion of a single-channel dimension also allows the model to reduce unnecessary calculations.
- **CL_1-CL_2-M_1** The first set of hidden layers is made up of a maximum pooling layer with dimensions of [2×2]i and two sets of 64 convolutional filters with dimensions of [3×3×1]. The initial [160×160×1] input data are convolved and down-sampled into a [80×80×62] feature map in conjunction with the activation function ReLU.
- **CL_3-CL_4-M_2** When it comes to the second set of hidden layers, first extract the convolutional features of the feature map using two sets of 126 dimensional [3×3×62] convolution masks. After that, use the activation function ReLU. Ultimately, the feature map is transformed into a [40×40×126] feature map and a [2×2] max-pooling layer.
- **CL_5-CL_6-CL_7-M_3** The third hidden layer group, is made up of three layers with 254 convolutional filters, each of which is succeeded by a ReLU. The dimensions of the convolution masks are [3×3×126]. As such, the dimensions of [20×20×254] features are obtained through a 2-layered convolution employing [2×2] max-pooling for sampling reduction.
- **CL_8-CL_9-CL_{10}-M_4** In order to extract the convolutional features of the feature map and use the activation function ReLU, first use three sets of 510 dimensional [3×3×254] convolution masks for the fourth group of hidden layers. Lastly, utilizing the max-pooling layer with a dimension of [2×2], the feature map is converted into a feature map with a dimension of [10×10×510].
- **CL_{11}-CL_{12}-CL_{13}-M_5** A ReLU and maximal pooling layer with a size of [5×5] are positioned after 1022 convolutional filtering layers with a size of [3×3×510] to make up the fifth hidden layer group. The output of the feature map is converted into features with a dimension of [5×5×1022] after convolution and sampling reduction.
- **CL_{14}-FC_1:** The use a set of convolution masks with a size of [5×5×1022] to reduce the sample size and organize the feature map lacking cushioning for the final set of concealed layers. After that, the characteristic map is transformed into a [1×1×1022] one-dimensional array. The modified convolution method can preserve feature consistency when instead of flattening. Next, employ dropout normalization, a ReLU, and a layer that is completely connected. Furthermore, the 22% of concealed units are eliminated in order to lessen over fitting during training. This set of hidden layers produces an output feature map with the dimensions [1×1×1022].
- **OUT:** N neurons make up the resultant layer, where N is the total amount of different personalities or topics in the record. This step involves the use of a fully-connected Soft maximum layer, which outputs the "1-to-N" match probabilities for the subjects under consideration.

This work's building is denser thanks to the use of the activation function and ReLU than other vein algorithms that also use algorithms based on deep learning. These additions not only solved the slope dissolution issue but also successfully shortened both the training and testing times. However, this work developed with a slow rate of learning and performed forward propagation optimizer processing using Soft maximum and the optimizer developed by Adam in order to improve the accuracy of the experimental outcomes, the identification performance of the system, and variables situations. The ideal variables were found via ongoing evaluation and instruction to increase the initial algorithm's equilibrium and suitability for palm vein samples.

As previously indicated, the intended network was created especially to handle the finger vein images that the suggested system would produce. Results are presented in Section III. To evaluate its efficacy, its performance was examined in conjunction with three cutting-edge CNN architectures: VGG-16, InceptionV3 [17], and DenseNet201 [18]. These networks were chosen in part due to their excellent outcomes in tests conducted using the Image Network Large Scale Visual Recognition Challenge [19].

3: Examination as well as the outcomes of Experiments

This part assessed the suggested noncontact palm vein identification method's comprehension achievement. Using the information that was created set; we ran comprehensive tests and got good results as a whole.'

Contraction	Layer Type	Number of Filter	Size of Feature Map	Size of kernel	Number of stride
IN	Image Input Layer	-	160×160×1	-	-
CL1	Convolutional Layer-1	62	160×160×62	3×3	1×1
CL2	Convolutional Layer-2	62	160×160×62	3×3	1×1
M1	Max-Pooling Layer-1	1	80×80×62	2×2	2×2
CL3	Convolutional Layer-3	126	80×80×126	3×3	1×1
CL4	Convolutional Layer-4	126	80×80×126	3×3	1×1
M2	Max-Pooling Layer-2	1	40×40×126	2×2	2×2
CL5	Convolutional Layer-5	254	40×40×254	3×3	1×1
CL6	Convolutional Layer-6	254	40×40×254	3×3	1×1
CL7	Convolutional Layer-7	254	40×40×254	3×3	1×1
M3	Max-Pooling Layer-3	1	20×20×254	2×2	2×2
CL8	Convolutional Layer-8	510	20×20×510	3×3	1×1
CL9	Convolutional Layer-9	510	20×20×510	3×3	1×1
CL10	Convolutional Layer-10	510	20×20×510	3×3	1×1
M4	Max-Pooling Layer-11	1	10×10×510	2×2	2×2
CL11	Convolutional Layer-11	1022	10×10×1022	3×3	1×1
CL12	Convolutional Layer-12	1022	10×10×1022	3×3	1×1
CL13	Convolutional Layer-13	1022	10×10×1022	3×3	1×1
M5	Max-Pooling Layer-5	1	5×5×1022	2×2	2×2
CL14	Convolutional Layer-14	1022	1×1×1022	5×5	1×1
FC1	Fully-Connected Layer-1	-	1022×1	-	-
OUT	Output Layer	N×1	-	-	-

Table 1: Projected CNN Construction

3.1: Putting Together the Palm Vein Data Set

Users can place their palm over the NIR detector on the hardware ends to capture the vein structure electronically. In order to guarantee that the NIR light dispersed evenly over the palm area, study participants positioned their palm about 10 cm above the sensor. The hardware terminal's bottom was fixed with the NIR sensor and light source. Although palm vein detection is more difficult due to high intra-subject variance, it is convenient and uses a safe contactless setup. It has 600 palm vein images of left and right hands from various people in our database. Each image had 640 x 480 pixels and was an 8-bit black and white JPEG. Ten photos in total, five per side, were taken over the course of two discussions, with a month-long gap between all session's launching duration.

3.2: Implementation of the Proposed Method

The suggested approach was put into practice in a brand-new cloud environment using a Raspberry Pi. The PC had the following requirements: 32 GB of RAM, Nvidia GTX 1080 Ti, and Intel i7-8700 3.20 GHz processor. Python and C++ were utilized for coding. The CNN was trained and tested using Tensorflow and Keras, which were developed by Abadi et al. [20]. However, variable setting is essential during instruction for CNN-based systems. CNNs that have the wrong parameter settings may not function well. The suggested records was evaluated and instructed in two separate phases for this research. In this case, 10% of the sample set served as a validation set for the learned model's assessment. The batch size was set to 72 and the instruction evaluate was set to 0.0001 for the algorithm's variables. For the algorithm to achieve total and constant integration, 2500 training cycles were required.

3.3: Comparing Performance Effectiveness with Various CNN Models and Vein Recognition Techniques

The accuracy of recognition rate is a crucial safety measure for a one-to-many identification system. Greater amounts correspond to higher security and improved identification execution. However, palm vein images were extracted from various time periods in order to precisely assess the effectiveness of the approach suggested in this study. Testing took place during the following time. Thirty individuals had their left and right hands classified as distinct individuals for the purposes of this study; as a result, sixty classes were created.

In order to guarantee a thorough experimental analysis, the quantity of amplified samples could be examined. The comparison's assessment metric is the Correct Identification Rates (CIR), which is described as:

$$CIR = \frac{Number\ of\ correctly\ identified\ cases}{Number\ of\ total\ cases}$$

Method	Correct Identification Rate
VGG-16[16]	90.22%
Inception-v3[17]	93.34%
Densenet-201[18]	94.17%
Proposed modification	98.54%

Table 2: Evaluation with vein recognition methods

Methods	Correct Identification Rate
Mirmohamdsadeghi et al.[12]	92.19%
Zhou et al.[21]	94.21%
Das et al.[22]	95.58%
Proposed method	98.54%

Table 3: Evaluation with condition of the skill CNN models

The conclusions obtained with different CNN algorithms are compared in Table II. Three cutting-edge CNN designs were compared to the suggested structure.

Specifically, DenseNet-201, Inception-v3, and VGG-16. The suggested improved CNN had the best recognition precision, as shown in Table II. The adjusted CNN algorithm's precision was 8% greater than the VGG-16 model's.

Additionally, Table III shows the outcomes of comparisons between various vein understanding techniques. The outcomes show that in the non-contact data set, the suggested palm vein identification method performs better.

4: CONCLUSIONS

In this study, a developed CNN-based palm vein identification system and used the Raspberry Pi operating system and cloud computing platform to build the device prototype. The suggested method successfully identified palm veins without physical contact. The outcomes of the experiment showed that the suggested system was able to identify objects with a high degree of accuracy (more than 98.5%) across a range of databases. The suggested strategy outperformed systems described in recent studies in terms of identification rate.

5: REFERENCES

1. X. Yin, X. Yu, K. Sohn, X. Liu, and M. Chandraker, "Feature Transfer Learning for Face Recognition With Under-Represented Data," Proc. IEEE Conference on Computer Vision and Pattern Recognition (CVPR), pp. 5697–5706, June 2019.
2. K. Telegenov, Y. Tlegenov, and A. Shintemirov, "A Low-Cost Open-Source 3-D-Printed Three-Finger Gripper Platform for Research and Educational Purposes," IEEE Access, vol. 3, pp. 638–647, May 2015.
3. B. Zhang, W. Li, P. Qing, and D. Zhang, "Palm-Print Classification by Global Features," IEEE Transactions on Systems, Man, and Cybernetics: Systems, vol. 43, no. 2, pp. 370–378, Mar. 2013.
4. C. Wang, J. Muhammad, Y. Wang, Z. He, and Z. Sun "Towards Complete and Accurate Iris Segmentation Using Deep Multi-Task Attention Network for Non-Cooperative Iris Recognition," IEEE Transactions on Information Forensics and Security, vol. 15, pp. 2944–2959, Mar. 2020.
5. F. Ahmad, L. Cheng, and A. Khan, "Lightweight and Privacy-Preserving Template Generation for Palm-Vein-Based Human Recognition," IEEE Transactions on Information Forensics and Security, vol. 15, pp. 184–194, May. 2020.
6. C. Lin, and K. Fan, "Biometric Verification Using Thermal Images of Palm-Dorsa Vein Patterns," IEEE Transactions on Circuits and Systems for Video Technology, vol. 14, no. 2, pp. 199–213, Feb. 2004.

7. K. Toh, H. Eng, Y. Choo, Y. Cha, W. Yau, and K. Low, "Identity Verification Through Palm Vein and Crease Texture," Proc. International Conference on Biometrics, pp. 546–553, Oct. 2005.
8. Y. Zhang, Q. Li, J. You, and P. Bhattacharya, "Palm Vein Extraction and Matching for Personal Authentication," Proc. International Conference on Visual Information Systems, pp. 154–164, 2007.
9. J. Lee, "A Novel Biometric System Based on Palm Vein Image," Pattern Recognition Letters, vol. 33, no. 12, pp. 1520–1528, Sep. 2012.
10. D. Han, Z. Guo, and D. Zhang, "Multispectral Palmprint Recognition Using Wavelet-Based Image Fusion," Proc. International Conference on Signal Processing, pp. 2074–2077, Oct. 2008.
11. P. Ladoux, C. Rosenberger, and B. Dorizzi, "Palm Vein Verification System Based on SIFT Matching," Proc. International Conference on Biometric, pp. 1290–1298, June 2009.
12. L. Mirmohamadsadeghi, and A. Drygajlo, "Palm Vein Recognition with Local Texture Patterns," IET Biometrics, vol. 3, no. 4, pp. 198–206, Dec. 2014.
13. W. Kang and Q. Wu, "Contactless Palm Vein Recognition Using a Mutual Foreground-Based Local Binary Pattern," IEEE Transactions on Information Forensics and Security, vol. 9, no. 11, pp. 1974–1985, Nov. 2014.
14. X. Ma, X. Jing, H. Huang, Y. Cui and J. Mu, "Palm Vein Recognition Scheme Based on an Adaptive Gabor Filter," IET Biometrics, vol. 6, no. 5, pp. 325–333, Aug. 2017.
15. L. Chen, Y. Zhu, G. Papandreou, F. Schroff, and H. Adam, "Encoder-Decoder with Atrous Separable Convolution for Semantic Image Segmentation," arXiv:1802.02611v3 [cs.CV], 2018.
16. K. Simonyan and A. Zisserman, "Very Deep Convolutional Networks for Large-Scale Image Recognition," Proc. International Conference on Learning Representations (ICLR), May 2015.
17. C. Szegedy, V. Vanhoucke, S. Ioffe, J. Shlens, and Z. Wojna, "Rethinking the Inception Architecture for Computer Vision," Proc. IEEE Conference on Computer Vision and Pattern Recognition (CVPR), pp. 2818–2826, June 2016.
18. G. Huang, Z. Liu, K. Q. Weinberger, and L. van der Maaten, "Densely Connected Convolutional Networks," Proc. IEEE Conference on Computer Vision and Pattern Recognition (CVPR), vol. 1, pp. 2261–2269, July 2017.
19. A. Canziani, A. Paszke, and E. Culurciello, "An Analysis of Deep Neural Network Models for Practical Applications," arXiv:1605.07678v4 [cs.CV], 2016.
20.   M. Abadi, A. Agarwal, P. Barham, E. Brevdo, Z. Chen, C. Citro, G. S. Corrado, A. Davis, J. Dean, M. Devin, S. Ghemawat, I. Goodfellow, A. Harp, G. Irving, M. Isard, R. Jozefowicz, Y. Jia, L. Kaiser, M. Kudlur, J. Levenberg, D. Mané, M. Schuster, R. Monga, S. Moore, D. Murray, C. Olah, J. Shlens, B. Steiner, I. Sutskever, K. Talwar, P. Tucker, V. Vanhoucke, V. Vasudevan, F. Viégas, O. Vinyals, P. Warden, M. Wattenberg, M. Wicke, Y. Yu, and X. Zheng, "TensorFlow: Large-Scale Machine Learning on Heterogeneous Distributed Systems," arXiv:1603.04467v2 [cs.DC], 2016.
21. Y. Zhou and A. Kumar, "Human Identification Using Palm-Vein Images," IEEE Transactions on Information Forensics and Security, vol. 6, no. 4, pp. 1259–1274, Dec. 2011.
22. R. Das, E. Piciucco, E. Maiorana and P. Campisi, "Convolutional Neural Network for Finger- Vein-Based Biometric Identification," IEEE Transactions on Information Forensics and Security, vol. 14, no. 2, pp. 360–373, Feb. 2019.